Direct Lyapunov Control Technique for the Stable Operation of Multilevel Converter-Based Distributed Generation in Power Grid

Majid Mehrasa, Edris Pouresmaeil, *Member, IEEE*, and João P. S. Catalão, *Senior Member, IEEE*

***Abstract*—This paper deals with a control strategy of multilevel converter topologies for integration of distributed generation (DG) resources into the power grid. The proposed control plan is based on the direct Lyapunov control (DLC) technique, which is an appropriate tool for the analysis and definition of a stable operating condition for DG link in the power grid. The compensation of instantaneous variations in the reference current components in ac side and dc voltage variations of cascaded capacitors in dc side of the interfacing system is considered properly, which is the main contribution and novelty of this paper in comparison with other control methods. By utilization of the proposed control technique, DG can provide continuous injection of active power in fundamental frequency from the dispersed energy sources to the grid. In addition, reactive power and harmonic current components of nonlinear loads can be provided with fast dynamic response, by setting a multiobjective reference current component in the current loop of DLC-based model. Therefore, achieving sinusoidal grid currents in phase with load voltages are possible, while the required power from the load side is more than the maximum capacity of interfaced multilevel converter. Simulation results confirm the effectiveness of the proposed control strategy in DG technology during dynamic and steady-state operating conditions.**

***Index Terms*—Direct Lyapunov control (DLC), distributed generation (DG), energy management, multilevel converter.**

NOMENCLATURE

A. Indices

i	a, b, c.
j	$1, 2, \ldots, (n-1)$.

Manuscript received December 20, 2013; revised May 21, 2014 and July 20, 2014; accepted August 1, 2014. This work was supported in part by the European Regional Development Fund, European Union (EU), through the COMPETE Project, in part by the Portuguese Funds through the Fundação para a Ciência e a Tecnologia, under Project FCOMP-01-0124-FEDER-020282 and Project PEst-OE/EEI/LA0021/2013, and in part by the EU Seventh Framework Programme FP7/2007-2013 under Grant 309048. Recommended for publication by Associate Editor Marta Molinas.

AQ:1 M. Mehrasa is with the Department of Electrical and Computer Engineering, Babol Noshirvani University of Technology, Babol 47148-71167, Iran (e-mail: m.majidmehrasa@gmail.com).

E. Pouresmaeil is with the Centre for Smart Energy Solutions, University of Southern Denmark, Odense 5230, Denmark (e-mail: edp@iti.sdu.dk).

J. P. S. Catalão is with the University of Beira Interior, Covilha 6201-001, Portugal, Instituto de Engenharia de Sistemas e Computadores-Investigação e Desenvolvimento, Lisbon 1000-029, Portugal, and also with the Instituto Superior Técnico, University of Lisbon, Lisbon 1049-001, Portugal (e-mail: catalao@ubi.pt).

Color versions of one or more of the figures in this paper are available online at http://ieeexplore.ieee.org.

Digital Object Identifier 10.1109/JESTPE.2014.2346016

B. Abbreviations

CC	Capability curve.
DG	Distributed generation.
DLC	Direct Lyapunov control.
KVL	Kirchhoff's voltage law.
KCL	Kirchhoff's current law.
LPF	Low pass filter.
NPC	Neutral point clamped.
PCC	Point of common coupling.
PF	Power factor.
THD	Total harmonic distortion.
VSC	Voltage source converter.

C. Variables

i_{g_i}	Grid currents.
i_{l_i}	Load currents.
i_{c_i}	DG currents.
i_d	Current components d-axis.
i_q	Current components q-axis.
i_{dc}	DC current.
I_{dc}	Steady-state value of DC current.
$i_{c_d}^*$	Reference current of DG in d-axis.
$i_{c_q}^*$	Reference current of DG in q-axis.
i_{dh_n}	Load current components in harmonic frequencies.
I_{av_d}	Average value of instantaneous variation of $i_{c_d}^*$.
I_{av_q}	Average value of instantaneous variation of $i_{c_q}^*$.
e_{g_i}	Grid voltage.
e_i	Voltage at PCC.
e_m	Reference voltage vector at PCC.
e_d	Load voltage in d-axis.
e_q	Load voltage in q-axis.
v_{c_j}	DC-link voltages on the cascaded capacitors.
u_{eq_i}	Switching state function.
v_{c_s}	Desired voltage value of cascaded capacitors.
S_{ij}	Switching of transistors in each phase.

D. Parameters

R_c	Equivalent resistance of the ac filter, coupling. transformer, and connection cables.
L_c	Equivalent inductance of the ac filter, coupling. transformer, and connection cables.
R_g	Grid resistance up to the PCC.
L_g	Grid inductance up to the PCC.
c_j	Cascaded capacitors.

P_{DG} Reference active power of DG.
P_{max} Maximum active power of DG.
Q_{DG} Reference reactive power of DG.
Q_l Load reactive power.
ω Grid angular frequency.
α_j Constant coefficient of switching function in. dynamic state operation.
β_j Constant coefficient of switching function in. dynamic state operation.
f Fundamental frequency.
f_c Cutoff frequency.

I. Introduction

The concept of distributed generation (DG) consists of relatively small generation units that are located at or near the point of power consumption. Application of DG technology in the power grid can yield many benefits from both the grid and demand sides [1]–[3].

DG has the capability of being less costly, highly efficient, and reliable; it can simplify the generation of energy near the load center [4]. Therefore, DG can be considered as an efficient preference for the residential, commercial, and industrial costumer loads to provide a secure and low-cost electricity [5]. Sustainable energy resources are good options to empower the interfacing system in DG platforms. These sources of energy meet both the reducing energy demand from the utility grid and greenhouse gas emissions for the environmental regulations [6]. Power injection from DG to the grid during the peak of demand can optimize the energy consumption and reduce the stress from the grid's point of view, and decrease the cost of energy consumption from the customer's point of view [7]. But, increasing the number of DG units in the power grid can make some problems in the operation and power management in the whole network [8].

Generally, voltage source converters (VSC) are used as the heart of interfacing system between the DG source and the power grid, and multilevel converter topologies are a good tradeoff solution between the performance and cost in high-power systems. Compared with standard two-level converter topology, multilevel converter topologies offer great advantages such as lower harmonic distortion, lower voltage stress on converter connected loads, lower common-mode voltage, and less electromagnetic interference. Therefore, by reducing filtering requirements, they not only improve the efficiency of converters, but also increase the load power and the load efficiency by improving the load voltage with a lower harmonic content [9]–[11]. Nevertheless, the control complexity increases in multilevel converter-based DG, compared with the conventional converter-based scheme. Therefore, an efficient and cost-effective control technique is highly demanded for integration of DG resources into the power grid.

Several studies have been reported in the literature regarding the control of DG interfacing system for integration of renewable and nonrenewable energy sources to the grid [12]–[19].

Different issues regarding the integration of DG units into the distribution grid have been presented in [12], and some operational challenges such as voltage control, grid protection, and fault levels have been discussed. Some topologies and control techniques of converter-based DG are studied in [13], addressing the utilization of DG technology as a power quality enhancement device in the power grid. A control strategy is proposed in [14] to mitigate the impact of DG on the protection coordination. The proposed control technique can limit the injected current from the DG link according to the DG terminal voltage. The control algorithm presented in [15] can control the interfacing system as a voltage-controlled converter. The proposed control plan provides control over frequency and voltage at the point of common coupling (PCC); then, DG unit can work in both the grid connected and autonomous modes. A control plan for the multilevel converter-based DG has been presented in [16] for the integration of sustainable energy sources into the power grid. The application of this control technique is mainly based on the injection of harmonic current components and reactive power compensation from the renewable energy resources (i.e., wind and solar) in medium and high power systems. Different hardware implementations for the DG technology, control structures for the interfacing system, and control strategies under the fault conditions are addressed in [17]. Camacho *et al.* [18] discussed reference current generation in the control circuit loop of interfaced converter, under grid fault condition. The generated reference current can provide a flexible voltage support during the presence of any faults in the grid voltage. A PLL-less control technique for DG link is presented in [19]. By elimination of PLL from the control loop of DG, synchronization problems between the DG link and power grid can be resolved, and the control loop has a fast dynamic response to variations in the grid parameters. Some other control plans are also proposed for achieving a unity power factor (PF) in the utility grid by the integration of DG link to the network [20], [21]. In [22], a feedback linearization technique has been presented for the control of a three-level neutral-point-clamped (NPC) converter for compensation of harmonic current components of grid-connected loads. By the introduction of this control method, DG technology can be considered as an active power filter (APF) device in a power system. A control technique is developed in [23] for injection of harmonic current components generated by nonlinear loads. The proposed scheme is basically an energy-based Lyapunov control technique and provides a globally stable system. But, the authors did not consider the impacts of instantaneous variations of reference current components that highly contribute in the concept of global stability. Several other control algorithms have been proposed in the concept of DG technology, which in most of the presented works, a solution for a serious problem in the power grid has been proposed and discussed.

In this paper, authors are introducing a control strategy on the basis of the direct Lyapunov control (DLC) technique for defining a stable operating region of DG units and control of multilevel converter as the heart of the interfacing system between the DG sources and power grid. The impacts of instantaneous variations of reference current components in ac side, and dc voltage variations of cascaded capacitors in dc side of interfaced multilevel converter in operation of DG units are considered properly, which is an important section regarding the new contribution of this control method in comparison

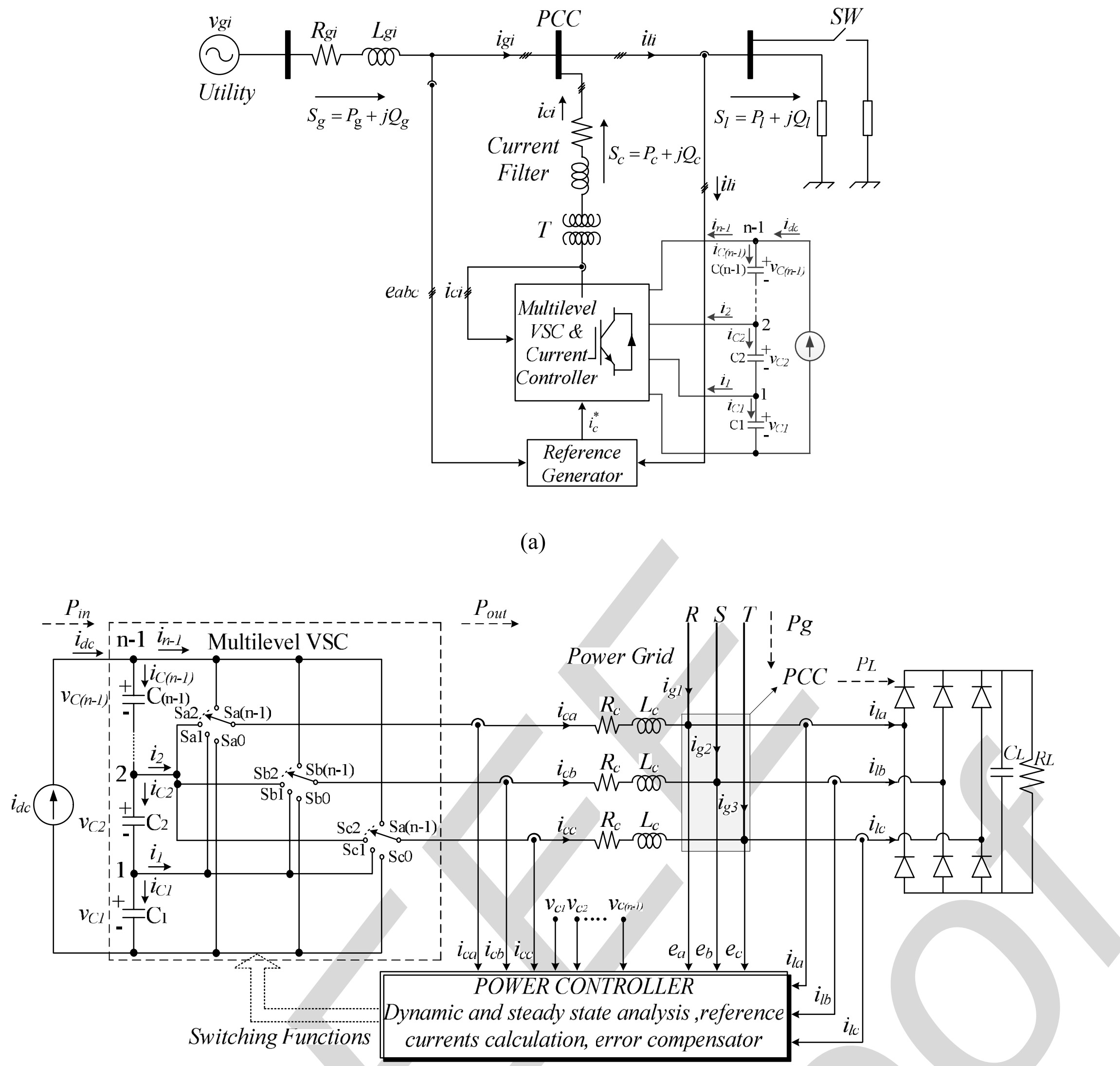

Fig. 1. Functional diagram of the proposed multilevel converter-based model. (a) Single-line diagram and (b) three-phase scheme.

with other potential control strategies. The contribution of this strategy in DG technology can be introduced as a solution in distribution grid, and the compensation for the different issues is needed concurrently during the connection of nonlinear loads.

The rest of paper is organized into five sections. Following Section I, the general schematic diagram of the proposed DG model is introduced in Section III, and the dynamic and state-space analysis of this scheme are elaborated properly. Application of the DLC technique for the control and stable operation of DG interface system in transient and steady-state operating condition is presented in Section IV. Moreover, simulation results are performed to demonstrate the efficiency and applicability of the developed control strategy in Section V. Finally, conclusions are drawn in Section V.

II. Proposed Model Scheme

Fig. 1 shows the single-line and three-phase schematic diagrams of the proposed multilevel converter-based DG model, which is composed of three main parts, such as, grid, load, and DG link. As shown in Fig. 1(a), the proposed DG model is integrated to the grid in shunt connection type, which injects current components from the DG source into PCC. Conventional signs of voltage and current components are shown in detail in Fig. 1(b). In addition, the DG source and additional components are represented as a dccurrent source, which is connected to the dc side of the interfaced converter.

A. Dynamic Model in a-b-c Reference Frame

Dynamic analytical model of the proposed multilevel converter-based schema shown in Fig. 1 should be developed, to draw an appropriate control plan for controlling the integrated DG resources to the power grid. These equations can be obtained by applying the KVL law for the voltage at PCC and KCL law for the current in dc side of the interfaced converter as

$$L_c\frac{di_{c_a}}{dt}+R_c i_{c_a}-\left(S_{a1}-\frac{1}{3}\sum_{j=a}^{b,c}S_{j1}\right)v_{c_1}-\left(S_{a2}-\frac{1}{3}\sum_{j=a}^{b,c}S_{j2}\right)v_{c_2}$$
$$-\cdots\cdots-\left(S_{a(n-1)}-\frac{1}{3}\sum_{j=a}^{b,c}S_{(n-1)}\right)v_{c_{(n-1)}}+e_a=0$$
$$L_c\frac{di_{c_b}}{dt}+R_c i_{c_b}-\left(S_{b1}-\frac{1}{3}\sum_{j=a}^{b,c}S_{j1}\right)v_{c_1}-\left(S_{b2}-\frac{1}{3}\sum_{j=a}^{b,c}S_{j2}\right)v_{c_2}$$
$$-\cdots\cdots-\left(S_{b(n-1)}-\frac{1}{3}\sum_{j=a}^{b,c}S_{j(n-1)}\right)v_{c_{(n-1)}}+e_b=0$$
$$L_c\frac{di_{c_b}}{dt}+R_c i_{c_b}-\left(S_{c1}-\frac{1}{3}\sum_{j=a}^{b,c}S_{j1}\right)v_{c_1}-\left(S_{c2}-\frac{1}{3}\sum_{j=a}^{b,c}S_{j2}\right)v_{c_2}$$
$$-\cdots\cdots-\left(S_{c(n-1)}-\frac{1}{3}\sum_{j=a}^{b,c}S_{j(n-1)}\right)v_{c_{(n-1)}}+e_c=0$$
$$c_1\frac{dv_{c_1}}{dt}+\left(S_{a1}i_{c_a}+S_{b1}i_{c_b}+S_{c1}i_{c_c}\right)-i_{\mathrm{dc}}=0$$
$$c_2\frac{dv_{c_2}}{dt}+\left(S_{a2}i_{c_a}+S_{b2}i_{c_b}+S_{c2}i_{c_c}\right)-i_{\mathrm{dc}}=0$$
$$\vdots \qquad\qquad \vdots \qquad\qquad \vdots$$
$$c_{n-2}\frac{dv_{c_{(n-2)}}}{dt}+(S_{a(n-2)}i_{c_a}+S_{b(n-2)}i_{c_b}+S_{c(n-2)}i_{c_c})-i_{\mathrm{dc}}=0$$
$$c_{n-1}\frac{dv_{c_{(n-1)}}}{dt}-((1-S_{a(n-1)})i_{c_a}-(1-S_{b(n-1)})i_{c_b}-(1-S_{c(n-1)})i_{c_c})-i_{\mathrm{dc}}=0. \qquad (1)$$

By substituting the relation between the load voltages and switching state functions of multilevel converter in (1), voltage relation between the ac and dc sides of the interfacing system can be obtained as

$$v_i=\left(S_{i_1}-\frac{1}{3}\sum_{k=a}^{b,c}S_{k_1}\right)v_{c_1}+\left(S_{i_2}-\frac{1}{3}\sum_{k=a}^{b,c}S_{k_2}\right)v_{c_2}+\cdots+\left(S_{i_{(n-1)}}-\frac{1}{3}\sum_{k=a}^{b,c}S_{k_{(n-1)}}\right)v_{c_{(n-1)}}. \qquad (2)$$

By referring to (2), equivalent switching function for an n-level converter-based interfacing system can be expressed as

$$u_{\mathrm{eq}_{i1}}=-\left(S_{i_1}-\frac{1}{3}\sum_{k=a}^{b,c}S_{k1}\right)$$
$$u_{\mathrm{eq}_{i2}}=-\left(S_{i_2}-\frac{1}{3}\sum_{k=a}^{b,c}S_{k2}\right)$$
$$\vdots \qquad \vdots \qquad \vdots$$
$$u_{\mathrm{eq}_{i(n-1)}}=-\left(S_{i(n-1)}-\frac{1}{3}\sum_{k=a}^{b,c}S_{k(n-1)}\right). \qquad (3)$$

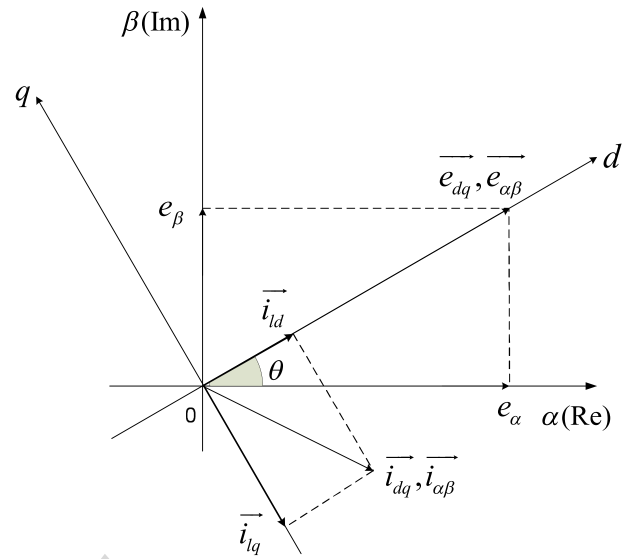

Fig. 2. Voltage and current components in special reference frames.

Equation (3) demonstrates that the equivalent switching functions of multilevel converter are depended on the switching of S_{ij}, completely describing the behavior of each leg in interfacing system. By substituting (3) in (1), the complete dynamic model of the propose scheme can be expressed based on the switching state function of interfaced converter as

$$L_c\frac{di_{c_a}}{dt}=-R_c i_{c_a}-u_{\mathrm{eq}_{a1}}v_{c_1}-u_{\mathrm{eq}_{a2}}v_{c_2}-\cdots\cdots-u_{\mathrm{eq}_{a(n-1)}}v_{c_{(n-1)}}-e_a$$
$$L_c\frac{di_{c_b}}{dt}=-R_c i_{c_b}-u_{\mathrm{eq}_{b1}}v_{c_1}-u_{\mathrm{eq}_{b2}}v_{c_2}-\cdots\cdots-u_{\mathrm{eq}_{b(n-1)}}v_{c_{(n-1)}}-e_b$$
$$L_c\frac{di_{c_b}}{dt}=-R_c i_{c_b}-u_{\mathrm{eq}_{c1}}v_{c_1}-u_{\mathrm{eq}_{c2}}v_{c_2}-\cdots\cdots-u_{\mathrm{eq}_{c(n-1)}}v_{c_{(n-1)}}-e_c$$
$$c_1\frac{dv_{c_1}}{dt}=u_{\mathrm{eq}_{a1}}i_{c_a}+u_{\mathrm{eq}_{b1}}i_{c_b}+u_{\mathrm{eq}_{c1}}i_{c_c}+i_{\mathrm{dc}}$$
$$c_2\frac{dv_{c_2}}{dt}=u_{\mathrm{eq}_{a2}}i_{c_a}+u_{\mathrm{eq}_{b2}}i_{c_b}+u_{\mathrm{eq}_{c2}}i_{c_c}+i_{\mathrm{dc}}$$
$$\vdots \qquad\qquad \vdots \qquad\qquad \vdots$$
$$c_{n-2}\frac{dv_{c_{(n-2)}}}{dt}=u_{\mathrm{eq}_{a(n-2)}}i_{c_a}+u_{\mathrm{eq}_{b(n-2)}}i_{c_b}+u_{\mathrm{eq}_{c(n-2)}}i_{c_c}+i_{\mathrm{dc}}$$
$$c_{n-1}\frac{dv_{c_{(n-1)}}}{dt}=u_{\mathrm{eq}_{a(n-1)}}i_{c_a}+u_{\mathrm{eq}_{b(n-1)}}i_{c_b}+u_{\mathrm{eq}_{c(n-1)}}i_{c_c}+i_{\mathrm{dc}}. \qquad (4)$$

B. Dynamic Model in dq Reference Frame

By use of the Park transformation matrix, the dynamic model of the whole system in (4) can be transformed into dq reference frame; therefore, all the ac variables of the proposed model in main frequency are converted to the dc value; consequently, controlling and filtering of the proposed DG model can be achieved easier.

Fig. 2 shows the voltage and current components in $\alpha\beta$ and dq reference frames [24]. Considering d-axis vector in the direction of reference voltage vector in this transformation, the q-component of reference voltage in rotating synchronous reference frame is always zero ($e_q = 0$) [19]. Therefore, the instantaneous angle of grid voltage can be calculated as

$$\theta = \tan^{-1} \frac{e_\beta}{e_\alpha}. \tag{5}$$

The grid voltage is considered ideal during the operation of the system; thus θ will not be involved with harmonic distortion, and consequently the obtained phase angle for dq transformation is proper in both steady and dynamic states.

As shown in Fig. 2, the magnitude of the voltage at PCC can be calculated as

$$e_m = |e_{dq}| = |e_{\alpha\beta}| = \sqrt{(e_\alpha)^2 + (e_\beta)^2}. \tag{6}$$

With the aforementioned considerations, the dynamic model of the proposed scheme can be expressed in dq frame as

$$\begin{aligned}
&L_c \frac{di_{c_d}}{dt} + R_c i_{c_d} - \omega L_c i_{c_q} + u_{\mathrm{eq}_{d1}} v_{c1} + u_{\mathrm{eq}_{d2}} v_{c2} \\
&\quad + \cdots\cdots + u_{\mathrm{eq}_{d(n-2)}} v_{c(n-2)} + u_{\mathrm{eq}_{d(n-1)}} v_{c(n-1)} + e_d = 0 \\
&L_c \frac{di_{c_q}}{dt} + R_c i_{c_q} + \omega L_c i_{c_d} + u_{\mathrm{eq}_{q1}} v_{c1} + u_{\mathrm{eq}_{q2}} v_{c2} \\
&\quad + \cdots\cdots + u_{\mathrm{eq}_{q(n-2)}} v_{c(n-2)} + u_{\mathrm{eq}_{q(n-1)}} v_{c(n-1)} + e_q = 0 \\
&C_1 \frac{dv_{c_1}}{dt} - (u_{\mathrm{eq}_{d1}} i_{c_d} + u_{\mathrm{eq}_{q1}} i_{c_q}) - i_{\mathrm{dc}} = 0 \\
&C_2 \frac{dv_{c_2}}{dt} - (u_{\mathrm{eq}_{d2}} i_{c_d} + u_{\mathrm{eq}_{q2}} i_{c_q}) - i_{\mathrm{dc}} = 0 \\
&\quad \vdots \qquad\qquad \vdots \qquad\qquad \vdots \\
&C_{n-1} \frac{dv_{c_{n-1}}}{dt} - \left(u_{\mathrm{eq}_{d(n-1)}} i_{c_d} + u_{\mathrm{eq}_{q(n-1)}} i_{c_q}\right) - i_{\mathrm{dc}} = 0.
\end{aligned} \tag{7}$$

Equation (7) illustrates the state-space model of the proposed multilevel converter-based DG scheme in dq frame, which is used for the dynamic and steady-state analysis of the whole model in the perspective control plan.

III. Proposed Control Technique

The proposed control technique in this paper is based on DLC algorithm, which is an appropriate technique for studying the stability of the proposed model in power grid. Through the proposed control technique, DG can be strengthened against the large signal disturbances and during the presence of unexpected changes in the loads of the proposed model.

A. Steady-State Evaluation in the Control Loop

Assuming that $i^*_{c_d}$ and $i^*_{c_q}$ are equilibrium points of the proposed DG in dq reference frame, if the reference current of $i^*_{c_d}$ is adjusted for the injection of the maximum active power in the fundamental frequency and total harmonic currents of nonlinear loads in d-axis into the grid through DG, the d-component of DG current in the closed-loop control can be expressed as

$$i_{c_d} = i^*_{c_d}. \tag{8}$$

Therefore, if the maximum active power of DG in fundamental frequency is more than the required active power from the load, the injected active power in fundamental and harmonic frequencies from the grid to the load will be zero. On the other hand, to generate the total reactive power through the proposed DG, $i^*_{c_q}$ should be considered as

$$i_{c_q} = i^*_{c_q}. \tag{9}$$

Two points can be understood from (9) that help to verify the accuracy of the sentence. First, (9) shows that DG guarantees all harmonic components of nonlinear load current in q reference frame, which leads to enhancing voltage quality. Second, (9) demonstrates that DG injects all q-component current of nonlinear load in fundamental frequency as well as all harmonic frequencies that cause the grid current including only d-component in fundamental frequency. It leads to unity PF in the grid. Moreover, voltage of load should be balanced and sinusoidal in the steady-state condition, therefore

$$e_d = e_m, e_q = 0. \tag{10}$$

Equations (8)–(10) are considered as the steady-state conditions in the proposed control plan. In addition, in the steady-state condition: $v_{c_1} = v_{c_2} = \cdots = v_{c_{(n-1)}} = v_{cs}$, $u_{\mathrm{eq}_{d1}} = u_{\mathrm{eq}_{d2}} = \cdots = u_{\mathrm{eq}_{d(n-1)}} = u_{\mathrm{eq}_{ds}}$ and $u_{\mathrm{eq}_{q1}} = u_{\mathrm{eq}_{q2}} = \cdots = u_{\mathrm{eq}_{q(n-1)}} = u_{\mathrm{eq}_{ds}}$.

When the capacitor voltages are aimed to reach different references, the steady-state conditions for output voltages will be $v_{c_i} = v_{cs_i}$, in which $v_{cs_i} \neq v_{cs_j}$ for $i \neq j, i$ and $j = 1, \ldots, n-1$. In this case, the midpoint of two adjacent capacitors draws significant current owing to their corresponding unequal voltages, which should be considered in a control strategy and is not the aim of the proposed controller. During the connection of linear loads to the grid, current components are only in fundamental frequency; then, the values of reference current components in dq frame are constant. But, during the connection of nonlinear loads to the grid, the presence of harmonic frequencies in the current components makes some variations in the reference current components, which may cause improper operation of the control loop and harmonic current injection from the interfaced converter to the grid. Then, these variations should be considered precisely for compensation in the control loop of the proposed DG model. In addition, θ is defined as the instantaneous angle of grid voltages in the previous section; then, the average values of instantaneous variations in the reference current components of DG control loop can be defined for compensation as

$$\frac{di^*_{c_d}}{dt} = I_{\mathrm{av}_d}, \frac{di^*_{c_q}}{dt} = I_{\mathrm{av}_q}. \tag{11}$$

Since the nonlinear load currents components in both d and q frame are not constant, the injected currents through DG will be variable. In this case, the derivative of d and q components currents of DG are obtained, which have specified values and are opposite of zero value. The obtained specified values are considered to exactly reach CC of DG and switching functions of the converter. By substituting (11) and applying the steady state conditions into (7), (12) can be obtained as

$$\begin{aligned}
L_c I_{\text{av}_d} + R_c i_{c_d}^* - \omega L_c i_{c_q}^* + (n-1) v_{cs} u_{\text{eq}_{ds}} + e_m &= 0\\
L_c I_{\text{av}_q} + R_c i_{c_q}^* + \omega L_c i_{c_d}^* + (n-1) v_{cs} u_{\text{eq}_{qs}} &= 0\\
u_{\text{eq}_{ds}} i_{c_d}^* + u_{\text{eq}_{qs}} i_{c_q}^* + I_{\text{dc}} &= 0\\
u_{\text{eq}_{ds}} i_{c_d}^* + u_{\text{eq}_{qs}} i_{c_q}^* + I_{\text{dc}} &= 0\\
\vdots \qquad\qquad \vdots \qquad\qquad &\vdots\\
u_{\text{eq}_{ds}} i_{c_d}^* + u_{\text{eq}_{qs}} i_{c_q}^* + I_{\text{dc}} &= 0\\
u_{\text{eq}_{ds}} i_{c_d}^* + u_{\text{eq}_{qs}} i_{c_q}^* + I_{\text{dc}} &= 0. \qquad (12)
\end{aligned}$$

According to (12), the switching state functions of interfaced multilevel converter for the steady-state operating condition can be expressed as

$$u_{\text{eq}_{ds}} = \frac{-R_c}{(n-1)v_{cs}} \left(\frac{L_c}{R_c} I_{\text{av}_d} + i_{c_d}^* - \frac{\omega L_c}{R_c} i_{c_q}^* + \frac{e_m}{R_c} \right) \qquad (13)$$

$$u_{\text{eq}_{qs}} = \frac{-R_c}{(n-1)v_{cs}} \left(\frac{L_c}{R_c} I_{\text{av}_q} + i_{c_q}^* + \omega \frac{L_c}{R_c} i_{c_d}^* \right). \qquad (14)$$

Equations (13) and (14) can be used for the desired control of DG in the steady-state condition by proper selection of $i_{c_d}^*$ and $i_{c_q}^*$. Each DG model has a limited capacity for the injection of active and reactive power, so considering the capacity of DG in design of control loop for the interfacing system can help to improve the performance of DG model in the distribution grid. By substituting (13) and (14) in *dc* part of (12), (15) can be obtained as

$$\left(i_{c_d}^* + \frac{L_c I_{\text{av}_d} + e_m}{2R_c} \right)^2 + \left(i_{c_q}^* + \frac{L_c I_{\text{av}_q}}{2R_c} \right)^2 = \frac{\left(L_c I_{\text{av}_d} + e_m\right)^2 + \left(L_c I_{\text{av}_q}\right)^2 + 4R_c(n-1)v_{cs} I_{\text{dc}}}{4R_c^2}. \qquad (15)$$

By multiplying e_m^2 to (15), (16) can be expressed as

$$\left(P_{\text{DG}} + \frac{L_c I_{\text{av}_d} e_m + e_m^2}{2R_c} \right)^2 + \left(Q_{\text{DG}} - \frac{L_c I_{\text{av}_q} e_m}{2R_c} \right)^2 = \frac{\left(L_c I_{\text{av}_d} e_m + e_m^2\right)^2 + \left(L_c e_m I_{\text{av}_q}\right)^2 + 4R_c(n-1)v_{cs} I_{\text{dc}} e_m^2}{4R_c^2}. \qquad (16)$$

Equation (16) is the equation of a circle with the center of $(-(L_c I_{\text{av}_d} e_m + e_m^2)/(2R_c), (L_c I_{\text{av}_q} e_m)/(2R_c))$ and radius of

$$e_m/2R_c \sqrt{\left(L_c I_{\text{av}_d} + e_m\right)^2 + \left(L_c I_{\text{av}_q}\right)^2 + 4R_c(n-1)v_{cs} I_{\text{dc}}}$$

which is shown in Fig. 3. This figure is considered as the capability curve (CC) of the proposed DG model, providing a proper division of active and reactive power between DG and the grid for supplying the load. As can be seen in Fig. 3, total reactive power of Load1 can be supplied through the DG link; but, after connection of Load2 to the grid, loads reactive power increases from Q_{11} to Q_{12}. As shown in this figure, total required power from the load side is not inside the circle, and it is more than the maximum capacity of interfaced converter for reactive power injection. Then, the rest of the active and reactive power will be supplied through the utility grid.

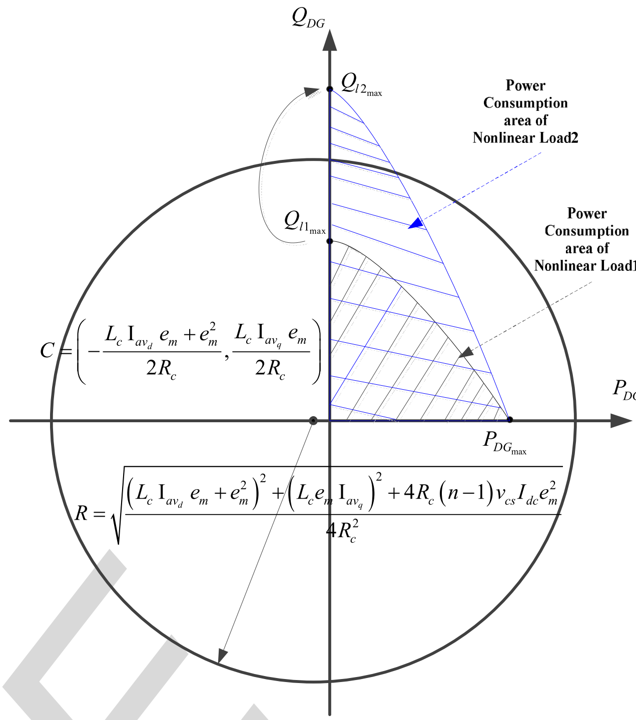

Fig. 3. Capability curve of the proposed DG scheme.

AQ:3

Therefore, DG can enhance the quality of grid current and PF between grid current and load voltage, while all the reactive power and harmonic current components of the load exist inside the circle of CC. In addition, DG can inject the total active power of the loads and reduce the grid current to zero value as long as the active power exists inside the circle.

B. Dynamic Evaluation of DLC Technique

Lyapunov function candidate $(E(x_1, x_2, \ldots, x_{n-1}, x_n, x_{n+1}))$ in the proposed DG scheme should be calculated to study the global stability of the proposed DG link through the DLC method and achieving dynamic parts of switching functions in the interfaced multilevel converter for proper integration of DG resources into the power grid. Thus

$$\begin{aligned}
E(x_1, x_2, \ldots, x_{n-1}, x_n, x_{n+1}) &= \frac{1}{2}L_c x_1^2 + \frac{1}{2}L_c x_2^2 + \frac{1}{2}C x_3^2 + \frac{1}{2}C x_4^2\\
&\quad + \cdots + \frac{1}{2}C x_{n-1}^2 + \frac{1}{2}C x_n^2 + \frac{1}{2}C x_{n+1}^2 \qquad (17)
\end{aligned}$$

where x_1 and x_2 are differences between the reference current components in the current control loop of DG and injected current through the interfaced multilevel converter to the grid $(i_{c_{dq}}^* \to i_{c_{dq}})$, and $x_3, x_4, \ldots, x_{n+1}$ are differences between the voltage of each cascaded capacitor, which is generated via the DG source, and desired dc voltages in dc side of the interfaced converter, compatible with the voltages at PCC $(v_{cj} \to v_{cs})$.

The globally asymptotical stability against the undesirable disturbances can be achieved for the proposed multilevel converter-based scheme, if the derivative of the defined Lyapunov function candidate in all the system in the state variables trajectories becomes definitive negative [25], [26].

By this assumption, total energy of the whole system tends to zero value and the condition for a stable operating system will be fulfilled. As a result (18) is given as

$$\frac{d}{dt}E(x_1, x_2, \ldots, x_n, x_{n+1}) = L_c x_1 \frac{dx_1}{dt} + L_c x_2 \frac{dx_2}{dt} + C x_3 \frac{dx_3}{dt} + \cdots + C x_n \frac{dx_n}{dt} + C x_{n+1} \frac{dx_{n+1}}{dt} < 0. \tag{18}$$

The switching state functions for the interfaced multilevel converter can be defined as

$$u_{\mathrm{eq}_{dq_j}} = u_{\mathrm{eq}_{dq_{js}}} + \Delta u_{\mathrm{eq}_{dq_j}} \tag{19}$$

where $\Delta u_{\mathrm{eq}_{dq_j}}$ is the dynamic part of the equivalent switching state function of interfaced multilevel converter. Equation (19) gives equivalent switching state functions of the interfaced converter, which is included in both dynamic and steady-state operating condition parts. By substituting steady-state conditions of variables and switching state functions of interfacing system, and (19) in (7), each dynamic part of (18) can be obtained as

$$\begin{aligned}
L_c \frac{dx_1}{dt} &= -R_c x_1 + \omega L_c x_2 - \frac{\left(-L_c I_{\mathrm{av}_d} - R_c i_{c_d}^* + \omega L_c i_{c_q}^* - e_m\right)}{(n-1)v_{cs}} \\
&\quad \times (x_3 + x_4 + \cdots + x_n + x_{n+1}) \\
&\quad - \Delta u_{\mathrm{eq}_{d1}} v_{c_1} - \Delta u_{\mathrm{eq}_{d2}} v_{c_2} \\
&\quad - \cdots\cdots - \Delta u_{\mathrm{eq}_{d(n-2)}} v_{c(n-2)} \\
&\quad - \Delta u_{\mathrm{eq}_{d(n-1)}} v_{c(n-1)} - e_m \\
L_c \frac{dx_2}{dt} &= -R_c x_2 - \omega L_c x_1 - \frac{\left(-L_c I_{\mathrm{av}_q} - R_c i_{c_q}^* - \omega L_c i_{c_d}^*\right)}{(n-1)v_{cs}} \\
&\quad \times (x_3 + x_4 + \cdots + x_n + x_{n+1}) \\
&\quad - \Delta u_{\mathrm{eq}_{q1}} v_{c_1} - \Delta u_{\mathrm{eq}_{q2}} v_{c_2} \\
&\quad - \cdots\cdots - \Delta u_{\mathrm{eq}_{q(n-2)}} v_{c(n-2)} - \Delta u_{\mathrm{eq}_{q(n-1)}} v_{c(n-1)} \\
c_1 \frac{dx_3}{dt} &= \frac{\left(-L_c I_{\mathrm{av}_d} - R_c i_{c_d}^* + \omega L_c i_{c_q}^* - e_m\right)}{(n-1)v_{cs}} x_1 + i_{\mathrm{dc}} - I_{\mathrm{dc}} \\
&\quad + \frac{\left(-L_c I_{\mathrm{av}_q} - R_c i_{c_q}^* - \omega L_c i_{c_d}^*\right)}{(n-1)v_{cs}} x_2 \\
&\quad + \Delta u_{\mathrm{eq}_{d1}} i_{c_d} + \Delta u_{\mathrm{eq}_{q1}} i_{c_q} \\
&\quad \vdots \qquad\qquad \vdots \qquad\qquad \vdots \\
c_{n-1} \frac{dx_{n+1}}{dt} &= \frac{\left(-L_c I_{\mathrm{av}_d} - R_c i_{c_d}^* + \omega L_c i_{c_q}^* - e_m\right)}{(n-1)v_{cs}} x_1 \\
&\quad + \frac{\left(-L_c I_{\mathrm{av}_q} - R_c i_{c_q}^* - \omega L_c i_{c_d}^*\right)}{(n-1)v_{cs}} x_2 \\
&\quad + \Delta u_{\mathrm{eq}_{d(n-1)}} i_{c_d} + \Delta u_{\mathrm{eq}_{q(n-1)}} i_{c_q} + (i_{\mathrm{dc}} - I_{\mathrm{dc}}).
\end{aligned} \tag{20}$$

By substituting the values of $(x_1, x_2, \ldots, x_{n-1}, x_n, x_{n+1})$ and the terms of (20), each part of (18) can be expressed as

$$\begin{aligned}
L_c x_1 \frac{dx_1}{dt} &= -R_c x_1^2 + \omega L_c x_2 x_1 - u_{\mathrm{eq}_{ds}} x_1 \\
&\quad \times (x_3 + x_4 + \cdots + x_n + x_{n+1}) \\
&\quad - \Delta u_{\mathrm{eq}_{d1}} x_1 v_{c_1} - \Delta u_{\mathrm{eq}_{d2}} x_1 v_{c_2} \\
&\quad - \cdots - \Delta u_{\mathrm{eq}_{d(n-2)}} x_1 v_{c(n-2)} \\
&\quad - \Delta u_{\mathrm{eq}_{d(n-1)}} x_1 v_{c(n-1)} - x_1 e_m \\
L_c x_2 \frac{dx_2}{dt} &= -R_c x_2^2 - \omega L_c x_1 x_2 - u_{\mathrm{eq}_{qs}} x_2 \\
&\quad \times (x_3 + x_4 + \cdots + x_n + x_{n+1}) \\
&\quad - \Delta u_{\mathrm{eq}_{q1}} x_2 v_{c_1} - \Delta u_{\mathrm{eq}_{q2}} x_2 v_{c_2} \\
&\quad - \cdots\cdots - \Delta u_{\mathrm{eq}_{q(n-2)}} x_2 v_{c(n-2)} \\
&\quad - \Delta u_{\mathrm{eq}_{q(n-1)}} x_2 v_{c(n-1)} \\
c_1 x_3 \frac{dx_3}{dt} &= u_{\mathrm{eq}_{ds}} x_1 x_3 + u_{\mathrm{eq}_{qs}} x_2 x_3 + \Delta u_{\mathrm{eq}_{d1}} x_3 i_{c_d} \\
&\quad + \Delta u_{\mathrm{eq}_{q1}} x_3 i_{c_q} + x_3 (i_{\mathrm{dc}} - I_{\mathrm{dc}}) \\
&\quad \vdots \qquad\qquad \vdots \qquad\qquad \vdots \\
c_{n-1} x_{n+1} \frac{dx_{n+1}}{dt} &= u_{\mathrm{eq}_{ds}} x_1 x_{n+1} + u_{\mathrm{eq}_{qs}} x_2 x_{n+1} \\
&\quad + \Delta u_{\mathrm{eq}_{d(n-1)}} x_{n+1} i_{c_d} + \Delta u_{\mathrm{eq}_{q(n-1)}} x_{n+1} i_{c_q} \\
&\quad + x_{n+1} (i_{\mathrm{dc}} - I_{\mathrm{dc}}).
\end{aligned} \tag{21}$$

By substituting different terms of (21) in (18), (22) can be expressed as

$$\begin{aligned}
&\frac{d}{dt}E(x_1, x_2, \ldots, x_n, x_{n+1}) \\
&= -R_c \left(i_{c_d} - i_{c_d}^*\right)^2 - R_c \left(i_{c_q} - i_{c_q}^*\right)^2 - \Delta u_{\mathrm{eq}_{d1}} \left(v_{cs} i_{c_d} - v_{c_1} i_{c_d}^*\right) \\
&\quad - \Delta u_{\mathrm{eq}_{d2}} \left(v_{cs} i_{c_d} - v_{c_2} i_{c_d}^*\right) \\
&\quad - \cdots - \Delta u_{\mathrm{eq}_{d(n-1)}} \left(v_{cs} i_{c_d} - v_{c(n-1)} i_{c_d}^*\right) \\
&\quad - \Delta u_{\mathrm{eq}_{q1}} \left(v_{cs} i_{c_q} - v_{c_1} i_{c_q}^*\right) - \Delta u_{\mathrm{eq}_{q2}} \left(v_{cs} i_{c_q} - v_{c_2} i_{c_q}^*\right) \\
&\quad - \cdots - \Delta u_{\mathrm{eq}_{d(n-1)}} \left(v_{cs} i_{c_d} - v_{c(n-1)} i_{c_d}^*\right) \\
&\quad - (i_{\mathrm{dc}} - I_{\mathrm{dc}}) \left(\left(v_{c_1} + v_{c_2} + \cdots + v_{c(n-2)} + v_{c(n-1)}\right) \right. \\
&\qquad \left. - (n-1) v_{cs}\right).
\end{aligned} \tag{22}$$

Equation (22) should have negative value to meet the criteria for globally asymptotical stability in the whole DG system during the dynamic changes in the proposed model. To reach this goal, dynamic parts of the switching state functions should be defined as

$$\Delta u_{\mathrm{eq}_{dj}} = \alpha_j \left(v_{cs} i_{c_d} - v_{c_j} i_{c_d}^*\right) \tag{23}$$

$$\Delta u_{\mathrm{eq}_{qj}} = \beta_j \left(v_{cs} i_{c_q} - v_{c_j} i_{c_q}^*\right). \tag{24}$$

Furthermore, v_{c_j} tends to be equal to v_{cs} for making an appropriate compatibility between the voltage of dc and ac sides during the integrating time; then, the last term in (22) will be eliminated and consequently the value of the general equation will be negative during the steady-state operating condition. But, during the transient time, two different conditions and values can be expected for v_{c_j} in comparison with v_{cs}.

At first condition, the value of v_{c_j} is assumed less than v_{cs}; then

$$\begin{aligned}
&\text{if } \left(v_{c_1} + v_{c_2} + \cdots + v_{c(n-2)} + v_{c(n-1)}\right) \\
&\qquad > (n-1) v_{cs} \Rightarrow i_{\mathrm{dc}} > I_{\mathrm{dc}} \\
&\text{then, } \left(v_{c_1} + v_{c_2} + \cdots + v_{c(n-2)} + v_{c(n-1)}\right) - (n-1) v_{cs} \\
&\qquad > 0 \text{ and } (i_{\mathrm{dc}} - I_{\mathrm{dc}}) > 0 \\
&\text{therefore, } (i_{\mathrm{dc}} - I_{\mathrm{dc}}) \left(\left(v_{c_1} + v_{c_2} + \cdots + v_{c(n-2)} + v_{c(n-1)}\right) \right. \\
&\qquad \left. - (n-1) v_{cs}\right) > 0.
\end{aligned} \tag{25}$$

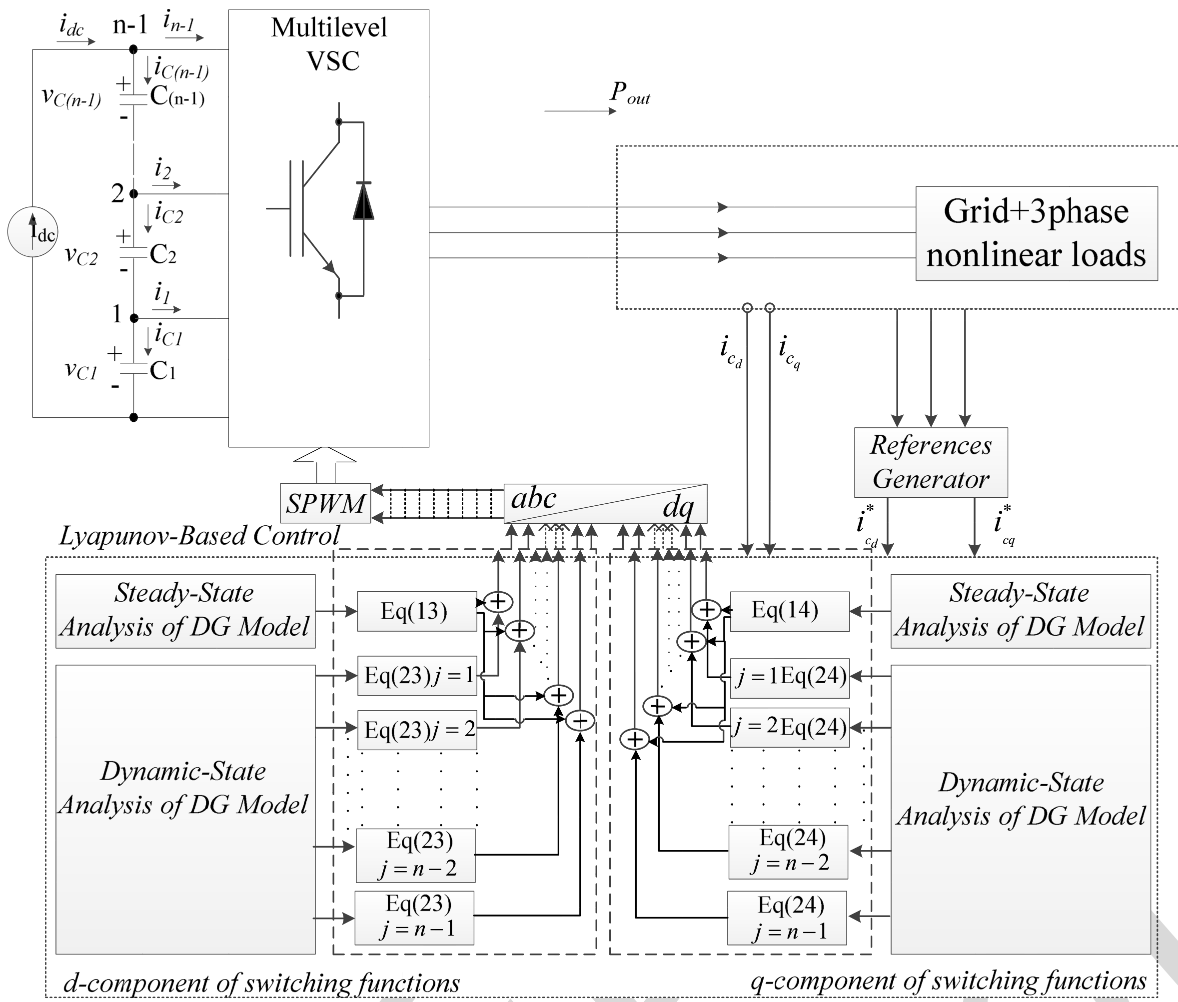

Fig. 4. Block diagram of DLC algorithm for the proposed DG model.

At second condition, the value of v_{c_j} is assumed greater than v_{cs}; then

$$\text{if } \left(v_{c_1} + v_{c_2} + \cdots + v_{c_{(n-2)}} + v_{c_{(n-1)}}\right) < (n-1)v_{cs} \Rightarrow i_{\text{dc}} < I_{\text{dc}}$$
$$\text{then } \left(v_{c_1} + v_{c_2} + \cdots + v_{c_{(n-2)}} + v_{c_{(n-1)}}\right) - (n-1)v_{cs} < 0 \text{ and } (i_{\text{dc}} - I_{\text{dc}}) < 0$$
$$\text{therefore } (i_{\text{dc}} - I_{\text{dc}})\left(\left(v_{c_1} + v_{c_2} + \cdots + v_{c_{(n-2)}} + v_{c_{(n-1)}}\right) -(n-1)v_{cs}\right) < 0. \tag{26}$$

As a result, application of DLC strategy can guarantee a stable operating region for the proposed multilevel converter-based DG scheme during the dynamic and steady-state operating conditions. The switching state functions of multilevel converter, given in (23) and (24), make a rapid reaction for the proposed control technique, and therefore, DG currents follow their reference values with a fast dynamic response in a stable operating region. The process of switching function generation in DLC technique is shown in Fig. 4.

C. Reference Current Calculation

Current reference values should be defined based on the objectives of DLC technique for an efficient operation during the dynamic and steady-state operating conditions. Therefore, the harmonic current components, maximum active power, and all the reactive power should be considered in the control loop of the proposed DG model. By this consideration and based on Fig. 3, the rest of the power for the additional load which will be injected from the utility grid is an active power in the fundamental frequency.

The instantaneous complex load power is defined as the product of the load voltage vector and the conjugate of the load current vector, given in the form of complex numbers. As shown in Fig. 2, the instantaneous complex value of load power will be obtained by

$$S = ei^* = P_l + jQ_l = \frac{3}{2}(e_d + je_q)(i_{ld} - ji_{lq}) \tag{27}$$

AQ:4

$$S = \frac{3}{2}(e_d i_{ld} + e_q i_{lq}) + j(e_q i_{ld} - e_d i_{lq})$$

then

$$P_l = \frac{3}{2}(e_d i_{ld} + e_q i_{lq}), \text{ and } Q_l = \frac{3}{2}(e_q i_{ld} - e_d i_{lq}).$$

According to the mentioned assumptions in previous sections regarding $e_q = 0$, d-component of reference current in control loop of the proposed DG scheme can be achieved by doing the sum of maximum capacity of interfaced

TABLE I
SIMULATION PARAMETERS

Grid Voltage	380 rms V
dc-Voltage	1000 V
Main Frequency	50 Hz
Converter Resistance	0.1 Ω
Converter Inductance	0.45 mH
α_1, β_1	0.01
α_2, β_2	0.01
Switching Frequency	10kHz
P_{ref}	6.5 kW
Number of levels	n=3

multilevel converter for the injection of active power in main frequency and alternating terms of load current components in d-axis as

$$i_{c_d}^* = \frac{P_{\max}}{e_m} + \sum_{n=2}^{\infty} i_{d_{hn}} = \frac{P_{\rm DG}}{e_d} + i_{l_d}(1 - {\rm LPF}). \quad (28)$$

The alternating terms of load current components can be separated from the dc part by a low pass filter (LPF) to minimize the influence of the high pass filter (HPF) phase responses. Thus, a minimal phase HPF (MPHPF) can be obtained, and the transfer function of this LPF has the same order and cutoff frequency of HPF. So, the minimal phase HPF can be obtained by the difference between the input signal and the filtered one. The considered filter has a cutoff frequency $f_c = (f/2)(f = 50$ Hz), which promises the extraction of dc part from the nonlinear load currents. Furthermore, to compensate the load reactive power at fundamental and harmonic frequencies, DG must inject i_{l_q} as

$$i_{l_q} = -\frac{Q_l}{e_m} = -\frac{Q_{\rm DG}}{v_{pcc_d}} = i_{c_q}^*. \quad (29)$$

However, DG has a limitation in generating active and reactive powers and also nonlinear load currents in both fundamental frequency and harmonic components according to CC of DG, as shown previously in Fig. 3, which should be considered in the use of DG.

IV. RESULTS AND DISCUSSION

The proposed model shown in Fig. 1 has been simulated in MATLAB/Simulink to demonstrate the performance of the proposed DLC method in DG technology. The values of model parameters are given in Table I. A 13.27 kVA NPC VSC has been considered as the heart of the interfacing system between the DG source and the utility grid. It is assumed that the interfaced converter generates the maximum power of $P = 6.5$ kW at the main frequency, continuously. Unexpected connection of DG to the grid and load increment is considered to evaluate the accurate dynamic response of DLC technique in the proposed model. THD analysis of the grid current and analysis of PF between grid current and load voltage will be evaluated to illustrate the performance of the proposed control technique as a power quality enhancement device.

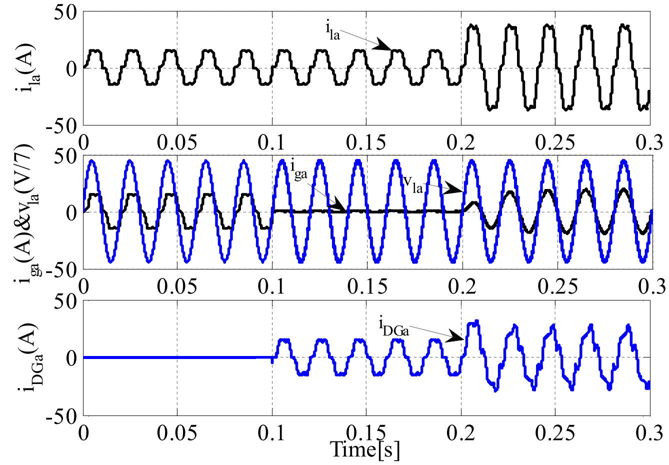

Fig. 5. Load, grid, and DG currents and load voltage, before and after DG interconnection, and before and after additional load increment.

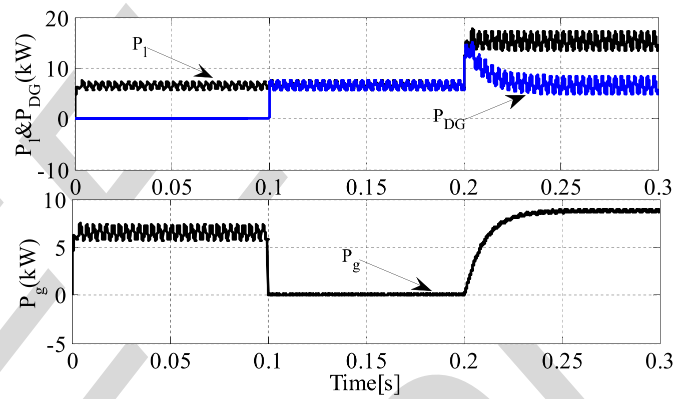

Fig. 6. Active power sharing between the load, DG, and grid before and after DG interconnection, and before and after additional load increment.

A. DG Connection and Load Increment

Before connection of DG link to the grid, a three-phase diode bridge rectifier with resistant load of $R = 30$ Ω is directly connected to the grid and draws the nonlinear currents from the grid. At $t = 0.1$ s, DG is connected to the grid and this procedure continues until $t = 0.2$ s, while another similar load with resistance of $R = 20$ Ω is added to the grid. Fig. 5 shows the load, grid, and DG currents before and after the connection of DG link to the grid, and after additional load increment.

As can be seen, before integration of DG to the grid, load is supplied by the utility grid. But, after connection of DG, all the current components including the fundamental and harmonic frequencies are injected by DG. After connection of the additional load to the grid at $t = 0.2$ s, the maximum capacity of multilevel converter is less than the total required power of the loads; then, the rest of the power which is active power in fundamental frequency is injected by the grid; therefore, load voltage and grid current are in phase during the connection of additional load to the grid.

Fig. 6 shows the active power sharing between the grid, load, and DG before and after integration of DG and before

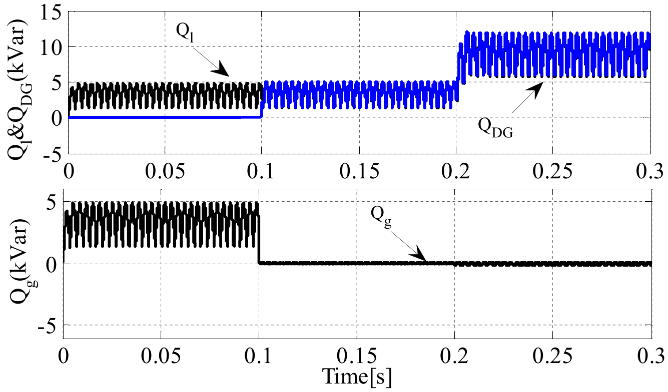

Fig. 7. Reactive power sharing between the load, DG, and grid before and after DG interconnection, and before and after additional load increment.

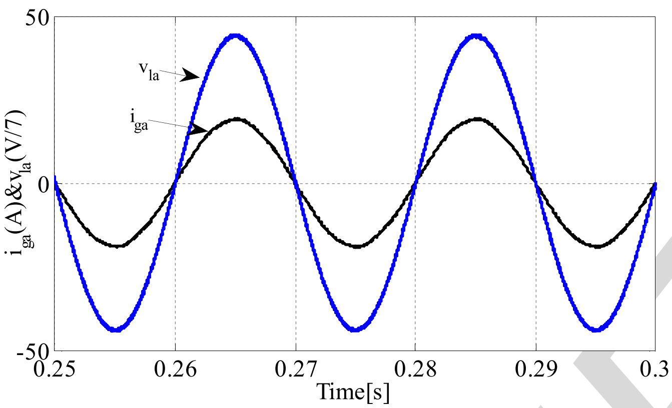

Fig. 8. Grid current and load voltage in phase (a), during load increment.

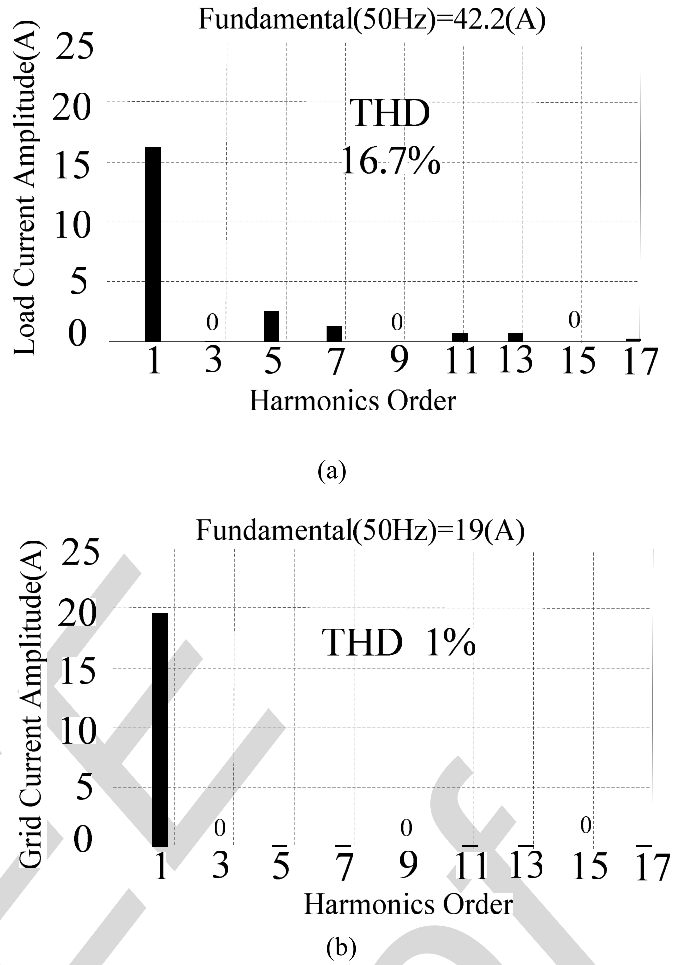

Fig. 9. Harmonic spectrum of load and grid current, during the additional load increment.

AQ:5

and after additional load increment. As shown in this figure, after connection of DG link to the grid, injected power from the grid reduced to the zero value and active power of load in both the fundamental and harmonic frequencies are supplied through the DG source. After connection of the additional load to the grid at $t = 0.2$ s, the maximum active power in fundamental frequency and all the harmonic current components are injected via the DG link, and the rest of the active power in fundamental frequency is supplied through the main grid.

Reactive power sharing between the grid, load and DG is shown in Fig. 7. As can be seen in this figure, all the reactive power in both the fundamental and harmonic frequencies are supplied via the DG link after connection of DG source to the grid and before and after connection of additional load to the grid; therefore, utility grid is free of any reactive power components and grid current is in phase with load voltage.

B. PF and THD Evaluation

One of the main objectives of the DLC strategy is to achieve a unit PF between the grid current and load voltage. To reach this goal, total load reactive power should be generated by DG. Fig. 8 shows the grid current and load voltage in phase (a) during the connection of additional load to the grid. As can be seen, grid current is in phase with load voltage, which confirms a unit value for the grid PF. Spectrum analysis results of the load and grid currents are shown in Fig. 9. As can be seen, THD of load current is 16.7% during connection of additional load to the grid, which could be the same value for the grid current during absence of DG link. But, by the interconnection of DG to the grid, THD of grid current is reduced to 1%, which confirms the capability of the proposed DG model to compensate the harmonic current components of nonlinear loads.

V. Conclusion

A control technique based on DLC method was presented in this paper for the control of multilevel converter topologies and integration of DG resources into the power grid. The compensation of instantaneous variations in the reference current components in ac side and dc voltage variations of cascaded capacitors in dc side of the interfacing system was considered properly as the main contribution and novelty of this control technique. Simulation results illustrated that in all conditions the maximum active power in fundamental frequency is injected through the DG link to the grid, and the load voltage and grid current are in phase by the injection of reactive power of loads in fundamental and harmonic frequencies via the DG link; then, DG can act as power factor correction device. In addition, the proposed DG can provide required harmonic current components of loads in all conditions. Therefore, by reducing the THD of the grid current, it can act as an active power filter. The proposed control method can be used for the integration of different types of DG resources, specially on the basis of renewable energy, as power quality enhancement device in a custom power distribution network.

REFERENCES

[1] P. Sotoodeh and R. D. Miller, "Design and implementation of an 11-level inverter with FACTS capability for distributed energy systems," *IEEE J. Emerg. Sel. Topics Power Electron.*, vol. 2, no. 1, pp. 87–96, Mar. 2014.

[2] Z. Liu and J. Liu, "Indirect current control based seamless transfer of three-phase inverter in distributed generation," *IEEE Trans. Power Electron.*, vol. 29, no. 7, pp. 3368–3383, Jul. 2014.

[3] Z. Liu, J. Liu, and Y. Zhao, "A unified control strategy for three-phase inverter in distributed generation," *IEEE Trans. Power Electron.*, vol. 29, no. 3, pp. 1176–1191, Mar. 2014.

[4] M. F. Shaaban, Y. M. Atwa, and E. F. El-Saadany, "DG allocation for benefit maximization in distribution networks," *IEEE Trans. Power Syst.*, vol. 28, no. 2, pp. 639–649, May 2013.

[5] I. Waseem, M. Pipattanasomporn, and S. Rahman, "Reliability benefits of distributed generation as a backup source," in *Proc. IEEE Power Energy Soc. General Meeting*, Jul. 2009, pp. 1–8.

[6] A. Mishra, D. Irwin, P. Shenoy, J. Kurose, and R. Misra, "GreenCharge: Managing renewable energy in smart buildings," *IEEE J. Sel. Areas Commun.*, vol. 31, no. 7, pp. 1281–1293, Jul. 2013.

[7] Y. Zhang, N. Gatsis, and G. B. Giannakis, "Robust energy management for microgrids with high-penetration renewables," *IEEE Trans. Sustain. Energy*, vol. 4, no. 4, pp. 944–953, Oct. 2013.

[8] F. Katiraei and M. R. Iravani, "Power management strategies for a microgrid with multiple distributed generation units," *IEEE Trans. Power Syst.*, vol. 21, no. 4, pp. 1821–1831, Nov. 2006.

[9] S. Kouro *et al.*, "Recent advances and industrial applications of multilevel converters," *IEEE Trans. Ind. Electron.*, vol. 57, no. 8, pp. 2553–2580, Aug. 2010.

[10] J. Rodriguez, S. Bernet, B. Wu, J. O. Pontt, and S. Kouro, "Multilevel voltage-source-converter topologies for industrial medium-voltage drives," *IEEE Trans. Ind. Electron.*, vol. 54, no. 6, pp. 2930–2945, Dec. 2007.

[11] E. Pouresmaeil, D. Montesinos-Miracle, and O. Gomis-Bellmunt, "Control scheme of three-level NPC inverter for integration of renewable energy resources into AC grid," *IEEE Syst. J.*, vol. 6, no. 2, pp. 242–253, Jun. 2012.

[12] E. J. Coster, J. M. A. Myrzik, B. Kruimer, and W. L. Kling, "Integration issues of distributed generation in distribution grids," *Proc. IEEE*, vol. 99, no. 1, pp. 28–39, Jan. 2011.

[13] Z. Zeng, H. Yang, R. Zhao, and C. Cheng, "Topologies and control strategies of multi-functional grid-connected inverters for power quality enhancement: A comprehensive review," *Renew. Sustain. Energy Rev.*, vol. 24, pp. 223–270, Aug. 2013.

[14] H. Yazdanpanahi, Y. W. Li, and W. Xu, "A new control strategy to mitigate the impact of inverter-based DGs on protection system," *IEEE Trans. Smart Grid*, vol. 3, no. 3, pp. 1427–1436, Sep. 2012.

[15] F. Gao and M. R. Iravani, "A control strategy for a distributed generation unit in grid-connected and autonomous modes of operation," *IEEE Trans. Power Del.*, vol. 23, no. 2, pp. 850–859, Apr. 2008.

[16] E. Pouresmaeil, O. Gomis-Bellmunt, D. Montesinos-Miracle, and J. Bergas-Jane, "Multilevel converters control for renewable energy integration to the power grid," *Energy*, vol. 36, no. 2, pp. 950–963, Feb. 2011.

[17] F. Blaabjerg, R. Teodorescu, M. Liserre, and A. V. Timbus, "Overview of control and grid synchronization for distributed power generation systems," *IEEE Trans. Power Electron.*, vol. 53, no. 5, pp. 1398–1409, Oct. 2006.

[18] A. Camacho, M. Castilla, J. Miret, J. C. Vasquez, and E. Alarcon-Gallo, "Flexible voltage support control for three-phase distributed generation inverters under grid fault," *IEEE Trans. Ind. Electron.*, vol. 60, no. 4, pp. 1429–1441, Apr. 2013.

[19] E. Pouresmaeil, C. Miguel-Espinar, M. Massot-Campos, D. Montesinos-Miracle, and O. Gomis-Bellmunt, "A control technique for integration of DG units to the electrical networks," *IEEE Trans. Ind. Electron.*, vol. 60, no. 7, pp. 2881–2893, Jul. 2013.

[20] F. D. Freijedo, J. Doval-Gandoy, O. Lopez, and E. Acha, "Tuning of phase-locked loops for power converters under distorted utility conditions," *IEEE Trans. Ind. Appl.*, vol. 45, no. 6, pp. 2039–2047, Nov./Dec. 2009.

[21] R. M. S. Filho, P. F. Seixas, P. C. Cortizo, L. A. B. Torres, and A. F. Souza, "Comparison of three single-phase PLL algorithms for UPS applications," *IEEE Trans. Ind. Electron.*, vol. 55, no. 8, pp. 2923–2932, Aug. 2008.

[22] E. Pouresmaeil, D. Montesinos-Miracle, O. Gomis-Bellmunt, and A. Sudria-Andreu, "Instantaneous active and reactive current control technique of shunt active power filter based on the three-level NPC inverter," *Eur. Trans. Elect. Power*, vol. 21, no. 7, pp. 2007–2022, Oct. 2011.

[23] S. Rahmani, A. Hamadi, and K. Al-Haddad, "A Lyapunov-function-based control for a three-phase shunt hybrid active filter," *IEEE Trans. Ind. Electron.*, vol. 59, no. 3, pp. 1418–1429, Mar. 2012.

[24] S. Naderi, E. Pouresmaeil, and W. D. Gao, "The frequency-independent control method for distributed generation systems," *Appl. Energy*, vol. 96, pp. 272–280, Aug. 2012.

[25] A. Isidori, *Nonlinear Control Systems*, 2nd ed. Berlin, Germany: Springer-Verlag, 1995.

[26] J. E. Slotine and W. Li, *Applied Nonlinear Control*. Englewood Cliffs, NJ, USA: Prentice-Hall, 1991.

Majid Mehrasa received the B.Sc. and M.Sc. degrees in electrical engineering from the University of Mazandaran, Babol, Iran, in 2006 and 2009, respectively.

He is currently a Lecturer with the University College of Rouzbahan, Sari, Iran. His current research interests include application of nonlinear control theories into multilevel converters, distributed generation, active power filter, and microgrid operation.

Edris Pouresmaeil (M'14) received the B.Sc. and M.Sc. degrees in electrical engineering from the University of Mazandaran, Babol, Iran, in 2003 and 2005, respectively, and the Ph.D. (Hons.) degree in electrical engineering from the Technical University of Catalonia, Barcelona Tech, Barcelona, Spain, in 2012.

He joined the Department of Electrical and Computer Engineering at the University of Waterloo, Waterloo, ON, Canada, as a Post-Doctoral Research Fellow, after the Ph.D. degree, and then joined the Department of Electromechanical Engineering at the University of Beira Interior, Covilha, Portugal. He is currently an Associate Professor with the Centre for Smart Energy Solutions, University of Southern Denmark, Odense, Denmark. His current research interests include power electronics converters for distributed generation, microgrids operation, integration of renewable energies in smart grids, and energy hub management system.

João P. S. Catalão (M'04–SM'12) received the M.Sc. degree from the Instituto Superior Técnico, Lisbon, Portugal, in 2003, and the Ph.D. and Habilitation degrees from the University of Beira Interior (UBI), Covilha, Portugal, in 2007 and 2013, respectively.

He is currently a Professor at UBI and a Researcher at INESC-ID, Lisbon. AQ:6 He is also the Primary Coordinator of the EU-funded FP7 project SiNGULAR. He has authored and co-authored more than 250 papers published in journals, book chapters, and conference proceedings, and has supervised more than 20 post-doctoral, Ph.D., and M.Sc. students. His current research interests include power system operations and planning, distributed renewable generation, demand response, and smart grids.

Prof. Catalão is an Editor of the IEEE TRANSACTIONS ON SMART GRID and the IEEE TRANSACTIONS ON SUSTAINABLE ENERGY, and an Associate Editor of the *IET Renewable Power Generation*. He is also an Editor of the book entitled *Electric Power Systems: Advanced Forecasting Techniques and Optimal Generation Scheduling* (CRC Press, 2012), and also translated into Chinese in 2014.